



DTC based on Fuzzy Logic Control of a Double Star Synchronous Machine Drive

D. Boudana¹, L. Nezli¹, A. Tlemçani¹, M.O. Mahmoudi¹
and M. Djemai^{2*}

¹ *Process Control Laboratory; Electrical Engineering Departement,
Ecole Nationale Polytechnique 10, avenue Hassen Badi, BP. 182, El-Harraech Algiers Algeria.*

² *LAMIH, UMR CNRS 8530, Université de Valenciennes et du Hainaut-Cambrésis,
Le Mont Houy, 59313 Valenciennes Cedex 9, France.*

Received: March 7, 2007; Revised: July 4, 2008

Abstract: The paper discusses a direct torque control (DTC) strategy based on a fuzzy logic for double star synchronous machine (DSSM). The DSSM is built with two symmetrical 3-phase armature winding systems, electrically shifted by 30°. A suitable transformation matrix is used to develop a simple dynamic model in view of control. The analysis of the torque in the stator flux linkage reference frame shows that the concept of DTC can be applied in DSSM. A set of voltage vectors corresponding to the switching mode are chosen to offer a maximum voltage and keep the harmonics at a minimum. Further, a switching table specific for DSSM is proposed. Simulations results are given to show the effectiveness and the robustness of our approach.

Keywords: *Double star synchronous machine (DSSM); direct torque control (DTC); fuzzy control; robustness; resistance stator estimator.*

Mathematics Subject Classification (2000): 34C60, 93D09, 93C42.

1 Introduction

AC machines with variable speed drives are widely employed in high power applications. In addition to the multilevel inverter fed electric machine drive systems ([4, 5]), one approach in achieving high power with rating limited power electronic devices is the multiphase inverter system. In a multiphase inverter fed machine, the windings of more than three phases are connected in the same stator of the machine, consequently the current per phase in machine is reduced [7, 19].

* Corresponding author: mohamed.djemai@ensea.fr

Multiphase machine possess several advantages over conventional three phase machine. These include increasing the inverter output power, reducing the amplitude of torque ripple and lowering the dc link current harmonics. Multiphase drive system improves the reliability, the motor can start and run since the loss of one or many phase [9]. For high power, the use of the synchronous machine specially finds its application in the motorisation at variable speed of the embedded systems [16]. But when they are supplied by thyristor current source inverter, torque ripples of high amplitude appear [23, 15]. Increasing the number of triple armature windings, witch is supplied in relation to each other one, lowers the rate of the torque ripples. Especially, the first harmonic of double star synchronous machine is twelve times the operating frequency of the machine [22].

During the last years, the modeling and control of double star synchronous machine has been the subject of investigations [20, 17, 21, 18, 1]. However the difficulty to control the DSSM supplied by two voltage source inverters (VSIs) is related to the fact that the model in Park frame is high order, multivariable and non linear. In [20] a monovariable approach in view of control of DSSM is proposed. This approach needs precise information about the parameters and rotor position of DSSM. A vector control method has been proposed to achieve a decoupling of rotor flux linkage and torque of DSSM in [16]. The proposed scheme used a rotor position and the torque was controlled via a stator current. One possible alternative to the vector control is the use of direct torque control strategies with several advantages based on possible control directly the stator flux linkage and the torque by selecting appropriate switching voltage vectors of the inverter. The method has been developed for electrical machines and first applied to induction motor drives and now, due to the availability of high-performance DSP process has resulted in the wide application of this technique in AC motor drives. The principle of a DTC consists to select stator voltage vectors according to the differences between the references of stator flux linkage and torque and their actual values. The DTC technique possesses advantages such as less parameter dependency, fast torque response and simple control scheme.

In this paper, we develop a DTC strategy based on a fuzzy logic ([6]) for double star synchronous machine to increase the system performances. A suitable transformation matrix is used to develop a simple dynamic model in view of control. A space vector decomposition control of VSIs fed DSSM is elaborated and DTC strategy is applied to get decoupled control of the flux and torque. In order to improve the static and dynamic control performance of the DSSM, the hysteresis controllers used in conventional DTC is replaced by a fuzzy controller. The main limitation of the DTC is the use the stator resistance for the estimation of stator flux. The variation of the stator resistance due to the temperature and frequency degrades the DTC controller performance especially at low speed. The DTC controller at low speed can be more reliable if the stator resistance is estimated on line and use it in the stator flux estimation algorithm. Several control schemes have been proposed to overcome this problem [8, 10, 14, 11]. To estimate the stator resistance we use a stator current error with PI estimator. The advantages of the proposed control system are shown by simulation involving 5kw DSSM.

2 Formulation Problem

The decoupled control scheme for double star synchronous machine supplied by two inverters is shown in Figure 2.1. The decoupled control bloc is based on DTC control

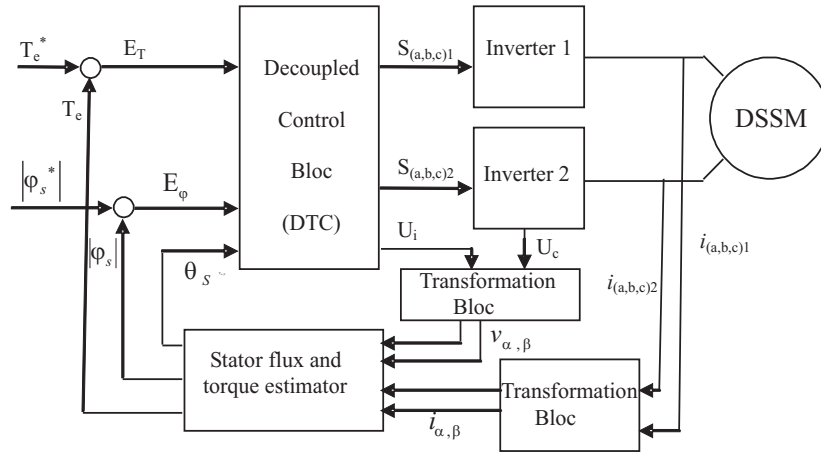


Figure 2.1: Decoupled control scheme for DSSM.

witch control the stator flux linkage and the torque directly, not via controlling the stator current.

2.1 Machine model

The studied system is a DSSM supplied by two VSIs (Figure 2.2). The DSSM is built with two symmetrical 3-phase armature winding systems, electrically shifted by 30° and its rotor is excited by constant current source (Figure 2.3).

In order to obtain a model of double star synchronous machine, we adopt the usual assumptions i.e.: the MMF in air-gap have a sinusoidal repartition and the saturation of the iron in machine is neglected [20, 1]. The stator voltage equation for six-phase can be written as:

$$[v_s] = [R_s] [i_s] + \frac{d}{dt} ([L_{ss}] [i_s] + [M_{sr}] i_f) \tag{1}$$

with

$$[v_s] = [v_{a1} \ v_{a2} \ v_{b1} \ v_{b2} \ v_{c1} \ v_{c2}]^T, \quad [i_s] = [i_{a1} \ i_{a2} \ i_{b1} \ i_{b2} \ i_{c1} \ i_{c2}]^T.$$

The original six dimensional system of the machine can be decomposed into three orthogonal subspaces (α, β) , (Z_1, Z_2) and (Z_3, Z_4) [1, 24]:

$$[F_\alpha \ F_\beta \ F_{Z1} \ F_{Z2} \ F_{Z3} \ F_{Z4}]^T = [T_s] [F_s], \tag{2}$$

where F_s can be voltage, courant or flux,

$$[T_s] = \frac{1}{\sqrt{3}} \begin{bmatrix} \cos(0) & \cos(\gamma) & \cos\left(\frac{2\pi}{3}\right) & \cos\left(\frac{2\pi}{3} + \gamma\right) & \cos\left(\frac{4\pi}{3}\right) & \cos\left(\frac{4\pi}{3} + \gamma\right) \\ \sin(0) & \sin(\gamma) & \sin\left(\frac{2\pi}{3}\right) & \sin\left(\frac{2\pi}{3} + \gamma\right) & \sin\left(\frac{4\pi}{3}\right) & \sin\left(\frac{4\pi}{3} + \gamma\right) \\ \cos(0) & \cos(\pi - \gamma) & \cos\left(\frac{4\pi}{3}\right) & \cos\left(\frac{\pi}{3} - \gamma\right) & \cos\left(\frac{2\pi}{3}\right) & \cos\left(\frac{5\pi}{3} - \gamma\right) \\ \sin(0) & \sin(\pi - \gamma) & \sin\left(\frac{4\pi}{3}\right) & \sin\left(\frac{\pi}{3} - \gamma\right) & \sin\left(\frac{2\pi}{3}\right) & \sin\left(\frac{5\pi}{3} - \gamma\right) \\ 1 & 0 & 1 & 0 & 1 & 0 \\ 0 & 1 & 0 & 1 & 0 & 1 \end{bmatrix}. \tag{3}$$

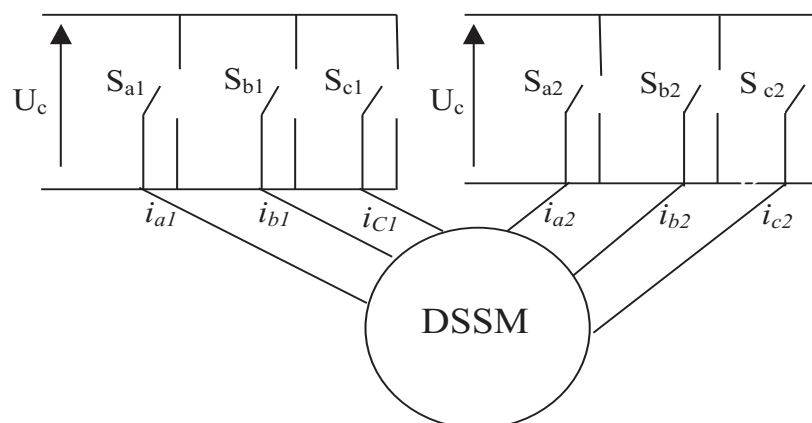


Figure 2.2: Electrical drive system.

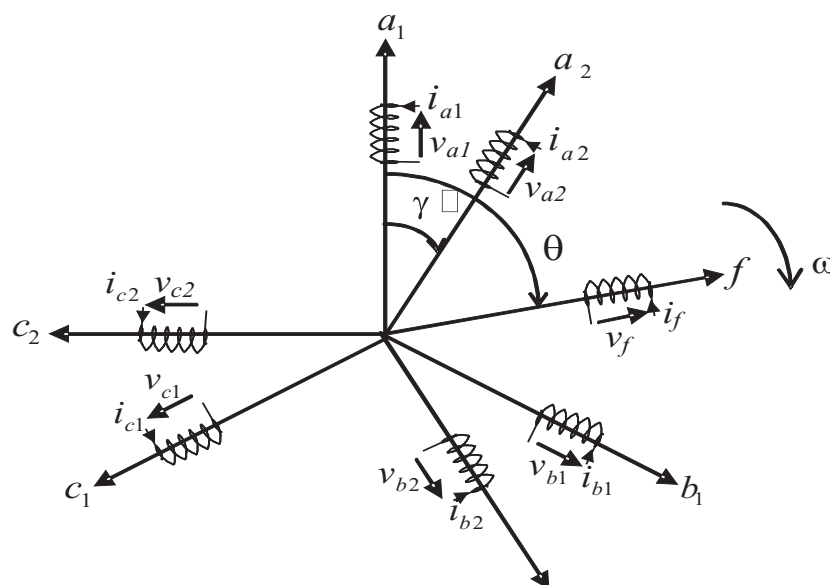


Figure 2.3: DSSM stator winding scheme.

From (1) and (2) the dynamic model describing the machine in $\alpha, \beta, Z_1, Z_2, Z_3, Z_4$ vector space can be given by

$$\begin{bmatrix} v_\alpha \\ v_\beta \\ v_{Z_1} \\ v_{Z_2} \\ v_{Z_3} \\ v_{Z_4} \end{bmatrix} = R_s \begin{bmatrix} i_\alpha \\ i_\beta \\ i_{Z_1} \\ i_{Z_2} \\ i_{Z_3} \\ i_{Z_4} \end{bmatrix} + \frac{d}{dt} \begin{bmatrix} l_{fs} + 3M_{ss} & 0 & 0 & 0 & 0 & 0 \\ 0 & l_{fs} + 3M_{ss} & 0 & 0 & 0 & 0 \\ 0 & 0 & l_{fs} & 0 & 0 & 0 \\ 0 & 0 & 0 & l_{fs} & 0 & 0 \\ 0 & 0 & 0 & 0 & l_{fs} & 0 \\ 0 & 0 & 0 & 0 & 0 & l_{fs} \end{bmatrix} \begin{bmatrix} i_\alpha \\ i_\beta \\ i_{Z_1} \\ i_{Z_2} \\ i_{Z_3} \\ i_{Z_4} \end{bmatrix} + M_{sfm} \frac{d}{dt} \begin{bmatrix} 3 \cos(2\theta) & 3 \sin(2\theta) & 0 & 0 & 0 & 0 \\ 3 \sin(2\theta) & -3 \cos(2\theta) & 0 & 0 & 0 & 0 \\ 0 & 0 & 0 & 0 & 0 & 0 \\ 0 & 0 & 0 & 0 & 0 & 0 \\ 0 & 0 & 0 & 0 & 0 & 0 \\ 0 & 0 & 0 & 0 & 0 & 0 \end{bmatrix} \begin{bmatrix} i_\alpha \\ i_\beta \\ i_{Z_1} \\ i_{Z_2} \\ i_{Z_3} \\ i_{Z_4} \end{bmatrix} + \sqrt{3}M_{sf} \frac{d}{dt} \begin{bmatrix} \cos(\theta) \\ \sin(\theta) \\ 0 \\ 0 \\ 0 \\ 0 \end{bmatrix} i_f.$$

It is observed from the above equations that all the electromechanical energy conversion related variable components are mapped into the α - β plane and the non electromechanical energy conversion related variable components are transformed to the Z_1, Z_2 and Z_3, Z_4 planes. Hence, the dynamic equations of the machine are totally decoupled. To express the stator and rotor equations in the same stationary reference frame, the following rotation transformation is appropriate

$$[P] = \begin{bmatrix} \cos(\theta) & -\sin(\theta) \\ \sin(\theta) & \cos(\theta) \end{bmatrix}.$$

With this transformation, the components of the α - β plane can be expressed in the d-q plan as

$$\begin{bmatrix} v_d \\ v_q \end{bmatrix} = \begin{bmatrix} R_s + pL_d & -\omega L_q \\ \omega L_d & R_s + pL_q \end{bmatrix} \begin{bmatrix} i_d \\ i_q \end{bmatrix} + M_d \omega \begin{bmatrix} 0 \\ 1 \end{bmatrix} i_f.$$

The electromagnetic torque of DSSM is expressed as

$$T_e = P(\varphi_d i_q - \varphi_q i_d)$$

with $\varphi_d = L_d i_d + M_{fd} i_f$; $\varphi_q = L_q i_q$; $L_d = l_{sf} + 3M_{ss} + 3M_{sfm}$; $L_q = l_{sf} + 3M_{ss} - 3M_{sfm}$; $M_d = \sqrt{3}M_{sf}$.

By applying the following rotation transformation, which transforms variable in the rotor flux reference frame ($d-q$) to the stator flux reference frame $x-y$ (Figure 2.4):

$$\begin{bmatrix} \cos(\delta) & -\sin(\delta) \\ \sin(\delta) & \cos(\delta) \end{bmatrix}.$$

The stator flux linkage and electromagnetic torque equations in $x-y$ reference frame are as follows [26]:

$$\begin{bmatrix} \varphi_x \\ \varphi_y \end{bmatrix} = \begin{bmatrix} L_d \cos^2 \delta + L_q \sin^2 \delta & -L_d \cos \delta \sin \delta + L_q \sin \delta \cos \delta \\ -L_d \cos \delta \sin \delta + L_q \sin \delta \cos \delta & L_d \sin^2 \delta + L_q \cos^2 \delta \end{bmatrix} \begin{bmatrix} i_x \\ i_y \end{bmatrix} + M_d \begin{bmatrix} \cos \delta \\ \sin \delta \end{bmatrix}, \tag{4}$$

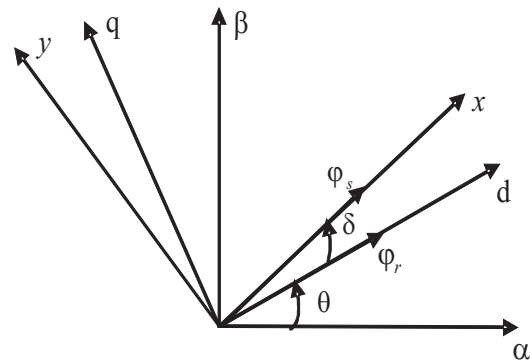


Figure 2.4: The stator and rotor flux linkages in different reference frames.

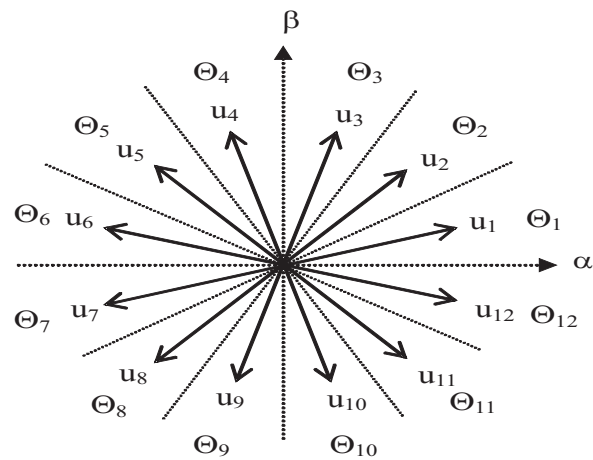


Figure 2.5: The chosen inverter voltage vectors projected on $\alpha - \beta$ plane.

$$T_e = P |\varphi_s| i_y.$$

The torque equation in terms of the stator flux linkage and load angle can be obtained by solving for i_y from the system equation (4) with $\varphi_y = 0$ and $\varphi_x = \varphi_s$, since the stator flux is along the x-axis [26]:

$$i_y = \frac{1}{2L_d L_q} [2M_d i_f L_q \sin \delta - |\varphi_s| (L_q - L_d) \sin 2\delta].$$

The torque equation is as follows:

$$T_e = \frac{P |\varphi_s|}{2L_d L_q} [2M_d i_f L_q \sin \delta - |\varphi_s| (L_q - L_d) \sin 2\delta]. \tag{5}$$

2.2 Modeling of the inverters

The DSSM is supplied by two VSIs. Each inverter can be controlled independently. However if we consider the two inverters as a six-phase voltage source inverter we obtain a total of 64 switching modes. By using the transformation matrix (3) the 64 voltage vectors corresponding to the switching modes are projected on three planes. From 64 vectors there are only 12 voltage vectors that offer a maximum voltage on the α - β plane and keep the harmonics on the Z_1, Z_2 plane at a minimum [24, 13].

The chosen switching modes are indicated in Table 2.1. The primary voltage $v_{a1}, v_{b1}, v_{c1}, v_{a2}, v_{b2}$ and v_{c2} are determined by the status of the six switches $S_{a1}, S_{b1}, S_{c1}, S_{a2}, S_{b2}, S_{c2}$. The non-zero voltage vectors are 30° apart from each other as in Figure 2.5.

$U[S_{a1}S_{b1}S_{c1}S_{a2}S_{b2}S_{c2}]$	$[v_{a1}v_{b1}v_{c1}v_{a2}v_{b2}v_{c2}].3/U_c$	$[v_\alpha v_\beta].1/U_c$
$u_1[1\ 0\ 0\ 1\ 0\ 0]$	$[2\ -1\ -1\ 2\ -1\ -1]$	$[1.077\ 0.288]$
$u_2[1\ 1\ 0\ 1\ 0\ 0]$	$[1\ 1\ -2\ 2\ -1\ -1]$	$[0.7887\ 0.7887]$
$u_3[1\ 1\ 0\ 1\ 1\ 0]$	$[1\ 1\ -2\ 1\ 1\ -2]$	$[0.2887\ 1.0774]$
$u_4[0\ 1\ 0\ 1\ 1\ 0]$	$[-1\ 2\ -1\ 1\ 1\ -2]$	$[-0.288\ 1.077]$
$u_5[0\ 1\ 0\ 0\ 1\ 0]$	$[-1\ 2\ -1\ -1\ 2\ -1]$	$[-0.788\ 0.288]$
$u_6[0\ 1\ 1\ 0\ 1\ 0]$	$[-2\ 1\ 1\ -1\ 2\ -1]$	$[-1.077\ 0.2887]$
$u_7[0\ 1\ 1\ 0\ 1\ 1]$	$[-2\ 1\ 1\ -2\ 1\ 1]$	$[-1.077\ -0.288]$
$u_8[0\ 0\ 1\ 0\ 1\ 1]$	$[-1\ -1\ 2\ -2\ 1\ 1]$	$[-0.788\ -0.788]$
$u_9[0\ 0\ 1\ 0\ 0\ 1]$	$[-1\ -1\ 2\ -1\ -1\ 2]$	$[-0.288\ -1.077]$
$u_{10}[1\ 0\ 1\ 0\ 0\ 1]$	$[1\ -2\ 1\ -1\ -1\ 2]$	$[0.288\ -1.077]$
$u_{11}[1\ 0\ 1\ 1\ 0\ 1]$	$[1\ -2\ 1\ 1\ -2\ 1]$	$[0.788\ -0.788]$
$u_{12}[1\ 0\ 0\ 1\ 0\ 1]$	$[2\ -1\ -1\ 1\ -2\ 1]$	$[1.077\ -0.288]$

Table 2.1: Chosen switching mode and primary voltage.

3 Direct Torque Control of DSSM

The main goal of DTC is to control the stator flux linkage and the torque directly, not via controlling the stator current. The change of torque can be controlled by keeping the amplitude of the stator flux linkage and by controlling the rotating speed of the stator flux linkage as fast as possible according to the equation (5).

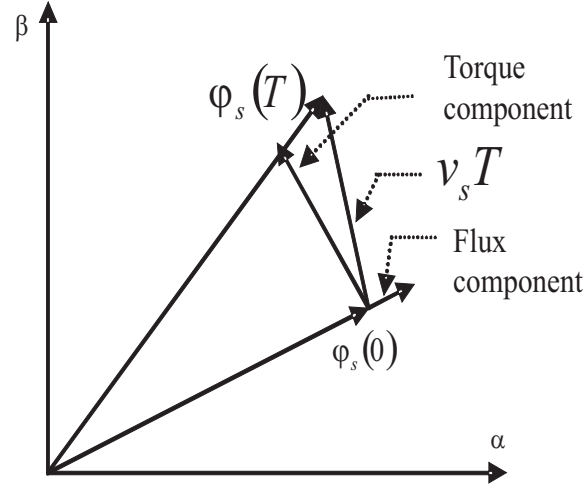


Figure 3.1: The control of stator flux linkage.

The stator flux linkage vector of DSSM in stationary reference frame is as follows:

$$\varphi_s(t) = \int_0^t (v_s - R_s i_s) dt + \varphi_s(0). \quad (6)$$

During the switching interval $[0 T]$, v_s is constant and equation (6) became:

$$\varphi_s(T) = v_s T - R_s \int_0^T i_s dt + \varphi_s(0).$$

It can be seen from the formula that the end of stator flux linkage vector φ_s will move along the direction of voltage vector applied if the stator resistance is neglected as shown in Figure 3.1.

The basic principle of the DTC is to select proper voltage vectors using a pre-defined switching table. The selection is based on the hysteresis control of the stator flux linkage and the torque [25, 3]. For example, in region Θ_1 , as shown in Figure 2.5, selection of vectors u_2, u_3 increases the amplitude of the stator flux linkage and increases torque. The selection of vectors u_4, u_5, u_6 decreases the amplitude of the stator flux linkage and increases torque. The selection of vectors u_8, u_9 decreases the amplitude of the stator flux linkage and decreases torque. The selection of vectors u_{10}, u_{11}, u_{12} increases the amplitude of the stator flux linkage and decreases torque. We have ten voltage vectors to control the amplitude of the stator flux linkage and torque, but with hysteresis controller we need only four voltage vectors to control the amplitude of the stator flux linkage and torque. The voltage vector plane is divided into twelve sectors so that each voltage vector divides each region into two equal parts as shown in Figure 2.5. In each sector, four of the twelve voltage vectors may be used. All possibilities can be tabulated into a switching table. The switching table used in this work is indicated in Table 3.1. The output of the flux hysteresis comparator is denoted as Φ , the output of the torque hysteresis comparator is denoted as τ . The flux hysteresis comparator is a two valued comparator. $\Phi=1$ means that the actual value of the amplitude of the flux linkage is below the reference value and

Φ	$\tau \setminus \Theta$	Θ_1	Θ_2	Θ_3	Θ_4	Θ_5	Θ_6	Θ_7	Θ_8	Θ_9	Θ_{10}	Θ_{11}	Θ_{12}
$\Phi = 1$	$\tau = 1$	u_3	u_4	u_5	u_6	u_7	u_8	u_9	u_{10}	u_{11}	u_{12}	u_1	u_2
$\Phi = 1$	$\tau = 0$	u_{11}	u_{12}	u_1	u_2	u_3	u_4	u_5	u_6	u_7	u_8	u_9	u_{10}
$\Phi = 0$	$\tau = 1$	u_5	u_6	u_7	u_8	u_9	u_{10}	u_{11}	u_{12}	u_1	u_2	u_3	u_4
$\Phi = 0$	$\tau = 0$	u_9	u_{10}	u_{11}	u_{12}	u_1	u_2	u_3	u_4	u_5	u_6	u_7	u_8

Table 3.1: The switching states for inverters.

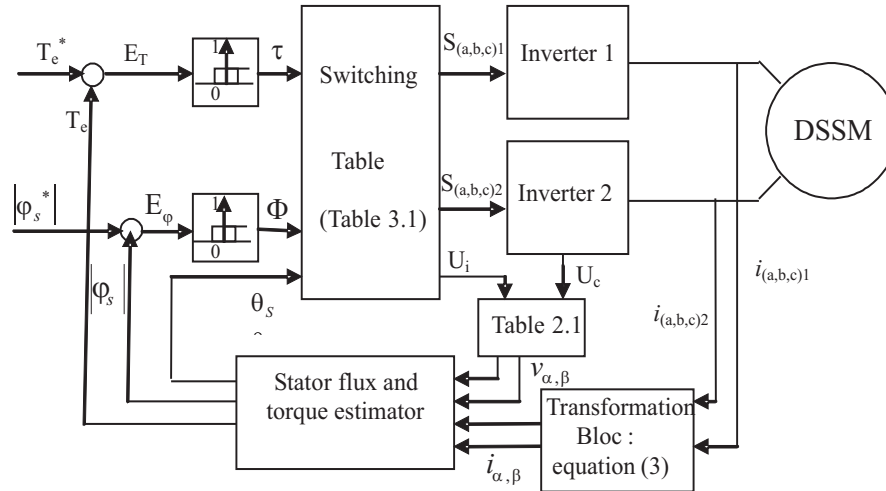


Figure 3.2: Direct torque control scheme for DSSM.

$\Phi=0$ means that the actual value is above the reference value. The same is true for the torque. Θ_i denote the region numbers for the stator linkage positions.

The used control system is depicted in Figure 3.2, E_T and E_φ are the torque and the flux errors.

The stator flux linkage and the torque are estimated with

$$\varphi_\alpha(t) = \int_0^t (v_\alpha - R_s i_\alpha) dt + \varphi_\alpha(0), \quad \varphi_\beta(t) = \int_0^t (v_\beta - R_s i_\beta) dt + \varphi_\beta(0),$$

$$|\varphi_s| = \sqrt{\varphi_\alpha^2 + \varphi_\beta^2}, \quad tg\theta_s = \frac{\varphi_\beta(t)}{\varphi_\alpha(t)}, \quad T_e = P(\varphi_\alpha i_\beta - \varphi_\beta i_\alpha).$$

The simulation results in Figure 3.3 show that basic DTC regulates the torque and stator flux well. We can see that, this control approach ensure good decoupling between stator flux linkage and torque. However, in this approach we have used only four voltage vectors to control flux and torque. In order to improve the performance of DSSM, we propose a DTC based on fuzzy logic to control flux and torque. In the proposed approach we used ten voltage vectors to control flux and torque.

4 The Proposed DTC Based on Fuzzy Logic for DSSM

In DTC scheme proposed in Section 3 a hysteresis controller is used. The output of hysteresis controller has only two states, which naturally leads to tacking the same action

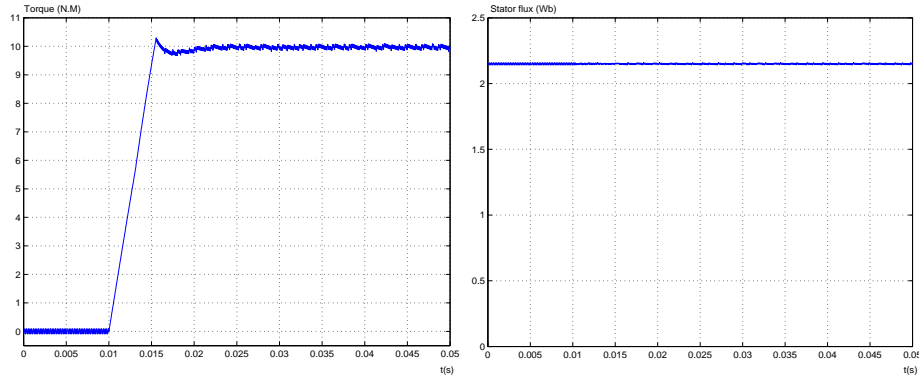


Figure 3.3: Performance of conventional DSSM DTC.

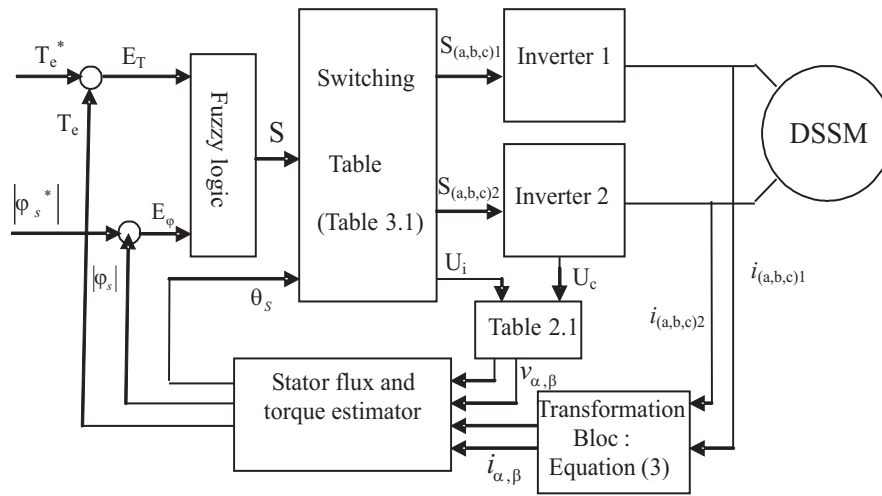


Figure 4.1: Direct torque control scheme based on fuzzy control for DSSM.

for the big torque error and small one. As consequence, a poor performances in response to step changes and large torque ripple. To improve the performances of DSSM, a DTC method based on a fuzzy control is used. The hysteresis controller is replaced by two input fuzzy controller and the vector output of the fuzzy controller is led to a switching table to decide which vector should be applied. This method has the advantage of fuzzy classification and has the advantage of simplicity and easy to implement [12]. The diagram of DTC incorporated with a fuzzy logic controller is shown in Figure 4.1. S denotes the vector output of the fuzzy controller.

4.1 Fuzzy controller

The fuzzy logic controller is comprised of fuzzification part, fuzzy inference part and defuzzification part.

A. Fuzzification.

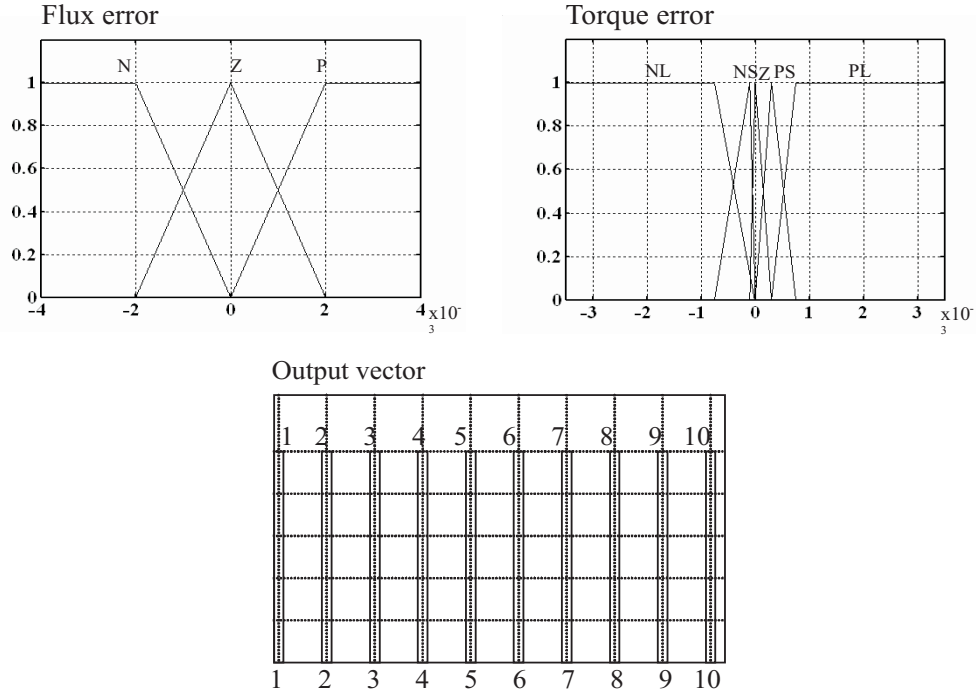


Figure 4.2: Membership function of fuzzy control.

The fuzzification is the process of a mapping from measured or estimated input to corresponding fuzzy set in the universe of discourse. As shown in Figure 4.1 there are two inputs E_φ and E_T . The member ship functions of the two fuzzy input variables are shown in Figure 4.2. The output variable can be classified into ten types, which are fuzzified as ten singleton fuzzy sets.

B. Fuzzy inference.

The fuzzy reasoning used is Mamdani’s method. The fuzzy control rule-base is shown in Table 4.1.

$E_T \setminus E_{\varphi_s}$	P	Z	N
PB	1	2	3
PS	4	2	5
NZ	-	-	-
NS	6	7	8
NB	9	7	10

Table 4.1: Fuzzy rule-bases.

Where 1,2,...,10 denote the specified states of the vector output of the fuzzy controller. Note that the above strategy was used in [12] for synchronous machine with four states of the vector output of the fuzzy controller.

C. Defuzzification.

The maximum criterion method is used for defuzzification. By this method, the value of fuzzy output which has the maximum possibility distribution is used as control output.

4.2 Selection of voltage vectors

The voltage vector, for controlling both the amplitude and rotating direction of φ_s , are indicated in Table 4.2.

$S \setminus \Theta$	Θ_1	Θ_2	Θ_3	Θ_4	Θ_5	Θ_6	Θ_7	Θ_8	Θ_9	Θ_{10}	Θ_{11}	Θ_{12}
$S = 1$	u_3	u_4	u_5	u_6	u_7	u_8	u_9	u_{10}	u_{11}	u_{12}	u_1	u_2
$S = 2$	u_4	u_5	u_6	u_7	u_8	u_9	u_{10}	u_{11}	u_{12}	u_1	u_2	u_3
$S = 3$	u_5	u_6	u_7	u_8	u_9	u_{10}	u_{11}	u_{12}	u_1	u_2	u_3	u_4
$S = 4$	u_2	u_3	u_4	u_5	u_6	u_7	u_8	u_9	u_{10}	u_{11}	u_{12}	u_1
$S = 5$	u_6	u_7	u_8	u_9	u_{10}	u_{11}	u_{12}	u_1	u_2	u_3	u_4	u_5
$S = 6$	u_{12}	u_1	u_2	u_3	u_4	u_5	u_6	u_7	u_8	u_9	u_{10}	u_{11}
$S = 7$	u_{10}	u_{11}	u_{12}	u_1	u_2	u_3	u_4	u_5	u_6	u_7	u_8	u_9
$S = 8$	u_8	u_{10}	u_{11}	u_{12}	u_1	u_2	u_3	u_4	u_5	u_6	u_7	u_8
$S = 9$	u_{11}	u_{12}	u_1	u_2	u_3	u_4	u_5	u_6	u_7	u_8	u_9	u_{10}
$S = 10$	u_9	u_{10}	u_{11}	u_{12}	u_1	u_2	u_3	u_4	u_5	u_6	u_7	u_8

Table 4.2: The switching states for inverters.

5 Comparative Study

In this section, we aim to compare the DTC based on fuzzy logic for DSSM to the conventional DTC for DSSM. We consider two situations:

Situation 1: Step change in torque. For the DTC based on fuzzy logic for DSSM we have simulated a step variation on the torque applied at $t=0.2$ ms. The obtained results are given in Figure 5.2, for the conventional DTC, see Figure 3.3. We can see that, both control approaches ensure good decoupling between stator flux linkage and torque. However the DTC based on fuzzy logic for DSSM decrease considerably the torque ripple and have faster torque response.

Situation 2: Stator resistance variation. For both DTC control schemes we have simulated variation on stator resistance as shown in Figure 5.5. The obtained results, shown in Figures 5.3 and 5.4, shows that the torque and flux are oscillating when stator resistance is increased. Thus incorrect resistance stator can causing instability. Several control scheme have been proposed to overcome this problem [8, 10, 14, 11]. The stator resistance estimator used in this paper is shown in Figure 5.1. The error in the stator current is used as an input to the PI estimator. The output of the PI estimator is continuously added to the previously estimated stator resistance.

\hat{i}_s the estimated stator current Figures 5.5, 5.6 and 5.7 shows the actual and estimated stator resistance and their error. We can see that the estimation error is approximately 0.02 % . In Figures 5.8 and 5.9 we have inserted the estimated stator resistance in control scheme. The obtained results are very satisfactory.

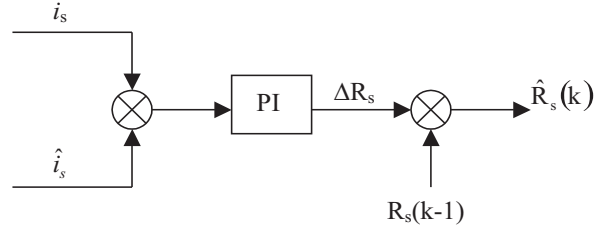


Figure 5.1: Block diagram of the stator resistance estimator.

	Torque ripple	Response time	Stator resistance variation
DTC based on fuzzy logic	0.4 %	4.5 ms	Unstable
Conventional DTC	2.4 %	10 ms	Unstable

Table 5.1: Comparative study between DTC based on fuzzy logic and conventional DTC for DSSM.

Table 5.1 summarizes the results of the comparative study. From the above table we can conclude that for the DSSM, the DTC based on fuzzy logic is more advantageous than the conventional DTC.

6 Conclusion

In this paper, we have developed a DTC for DSSM. First we have developed a conventional DTC for DSSM. In this approach we have used only four vectors voltage to control both torque and stator flux linkage. Secondly, in order to improve the performance of DSSM we have used ten vectors voltage to control torque and stator flux linkage. The proposed approach consist to replace the hysteresis controllers by two input fuzzy controller and the vector output of the fuzzy controller is led to a switching table to decide which vector should be applied. Thirdly, a comparative study demonstrates that the

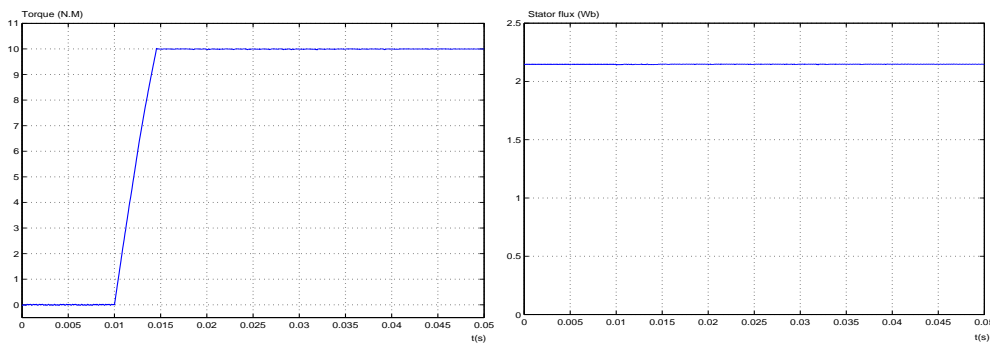


Figure 5.2: Performance of DSSM based on fuzzy control for situation 1.

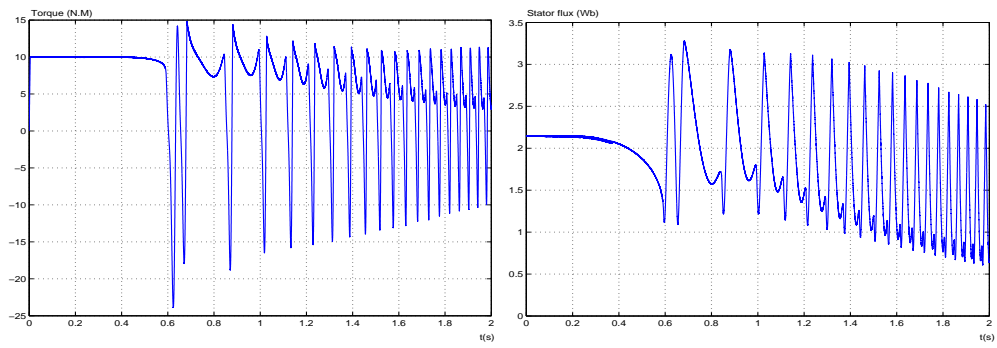


Figure 5.3: Performance of DSSM based on fuzzy control for situation 2.

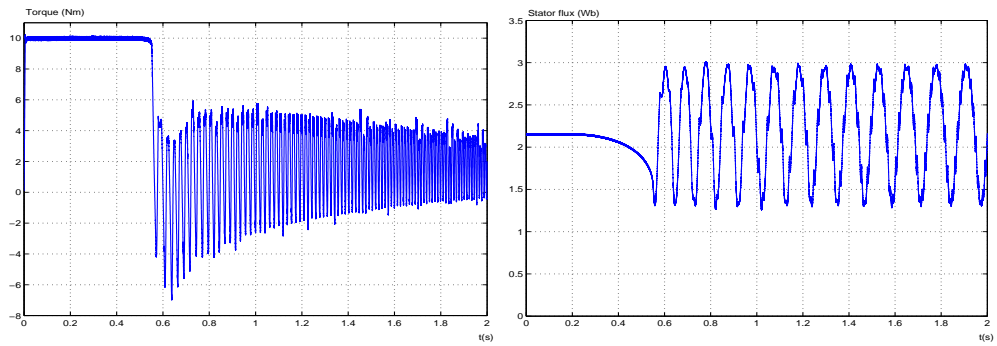


Figure 5.4: Performance of conventional DSSM DTC for situation 2.

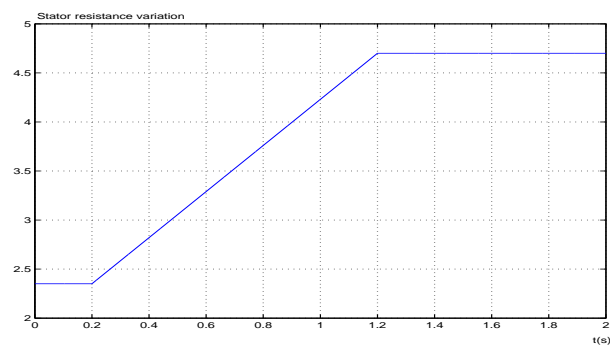


Figure 5.5: Actual stator resistance variation.

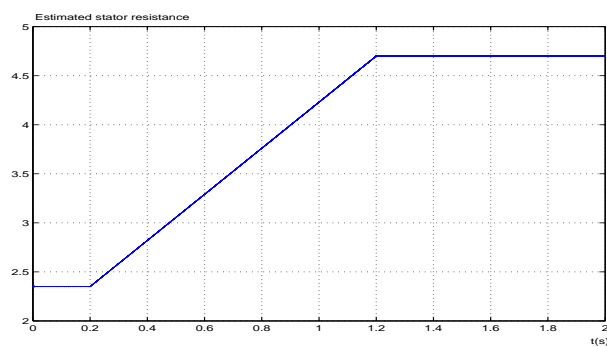


Figure 5.6: Estimated stator resistance.

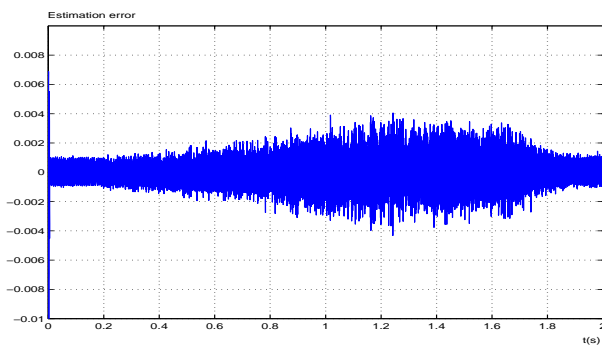


Figure 5.7: Estimation error.

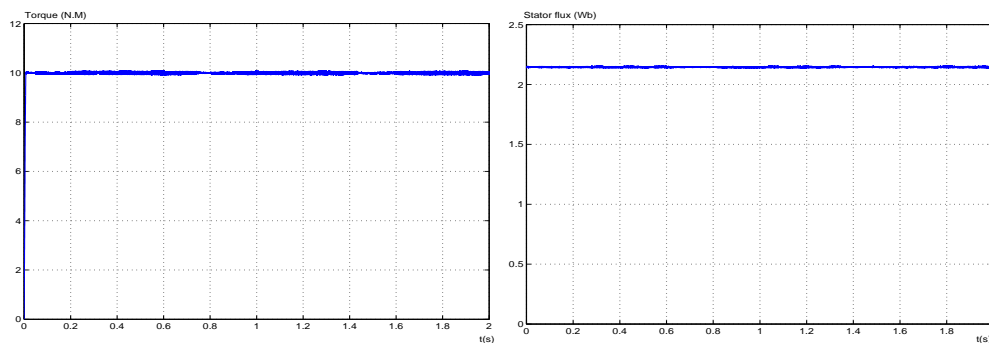


Figure 5.8: Performance of DSSM based on fuzzy control with estimated stator resistance.

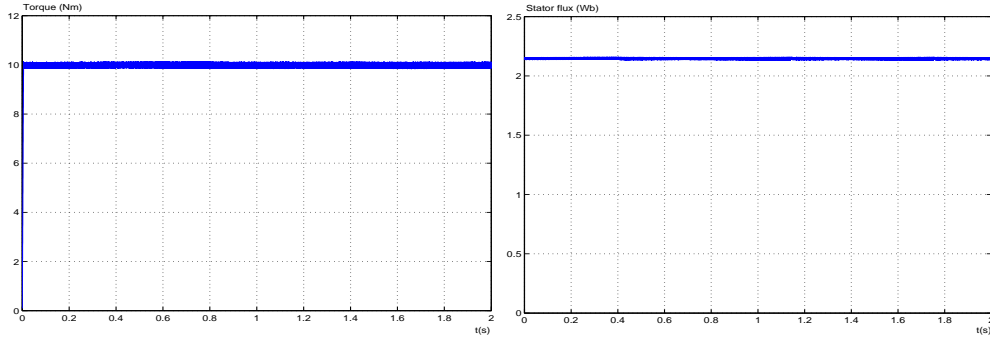


Figure 5.9: Performance of conventional DSSM DTC with estimated stator resistance.

DTC based on fuzzy logic for DSSM decrease the torque ripple and has a better dynamic and static performance. Nevertheless the variations of the stator resistance cause the DTC drive system to become unstable. So a PI stator resistance estimator is designed and applied to eliminate the effect of the stator resistance variation. It is shown that the stator flux and torque response is very satisfactory.

7 Appendix 1: List of Principal Symbols

v_{a1}, v_{b1}, v_{c1} : simple voltage of stator three phase first winding.

v_{a2}, v_{b2}, v_{c2} : simple voltage of stator three phase second winding.

i_{a1}, i_{b1}, i_{c1} : stator current a, b, c phase of first winding.

i_{a2}, i_{b2}, i_{c2} : stator current a, b, c phase of second winding.

i_s, \hat{i}_s : stator current vector, estimated stator current vector.

v_s : stator voltage vector.

v_d, v_q : stator voltages d-q axis.

v_α, v_β : stator voltages α - β axis.

v_x, v_y : stator voltages x-y axis.

$[L_{ss}]$: stator inductance matrix.

$[M_{sr}]$: stator-rotor mutual inductance matrix.

$[R_s]$: $\text{diag}(R_s, R_s, R_s, R_s, R_s, R_s)$.

R_s : stator resistance.

L_d, L_q : d-q inductances.

R_f : rotor resistance.

T_e, T_e^* : electromagnetic torque, reference torque.

φ_s, φ_s^* : stator flux vector, reference flux vector.

φ_d, φ_q : stator flux d-q axis.

$\varphi_\alpha, \varphi_\beta$: stator flux α - β axis.

φ_x, φ_y : stator flux x-y axis.

w : stator voltages synchronous pulsation.

Φ : output of the flux hysteresis comparator.

τ : output of the torque hysteresis comparator.

δ : angle between rotor and stator flux linkage.

θ_s : angle of stator flux linkage.

Θ_i : the region numbers for the stator linkage positions.

E_T : torque error.

E_φ : flux error.

J : friction coefficient.

f_r : moment of inertia.

P : pole pairs number.

7.1 Appendix 2: DSSM Parameters

$P_n = 5$ kW, $U_c = 232$ V, $i_f = 1$ A, $R_s = 2.35$ Ω , $R_f = 30.3$, $L_d = 0.3811$ H, $L_q = 0.211$ H, $L_f = 15$ H, $M_d = 2.146$ H, $J = 0.05$ Nms²/rd, $f_r = 0.001$ Nms/rd, $P = 1$.

References

- [1] Benkhoris, M.F., Merabtene, M., Meibody-Tabar, F., Davat, B. and Semail, E. Approches de modélisation de la machine synchrone double étoile alimentée par des onduleurs de tension en vue de la commande *RIGE* **6** (5-6) (2003) 579–608.
- [2] Bojoi, R., Farina, F., Griva, G., Profumo, F. and Tenconi, A. Direct Torque Control for Dual-Three Phase Induction Motor Drives *IEEE Transactions on Industry Applications* **41** (6) (2005) 1627–1636.
- [3] Buja, G.S. and Kazmierkowski, M.P. Direct torque control of PWM inverter-fed AC motors—a survey *IEEE Transaction on Industrial Electronics* **51** (4) (2004) 744–757.
- [4] Chekireb, H., Tadjine, M. and M. Djemaï. On a Class of Manifolds for Sliding Mode Control and Observation of Induction Motor. *Nonlinear Dynamics and Systems Theory* **8** (1) (2008) 21–34.
- [5] Chekireb, H., Tadjine, M. and M. Djemaï. Lyapunov Based on Cascaded Non-linear Control of Induction Machine. *Nonlinear Dynamics and Systems Theory* **7** (3) (2007) 225–252.
- [6] Chen, Y-H., Optimal Design of Robust Control for Uncertain Systems: a Fuzzy Approach. *Nonlinear Dynamics and Systems Theory* **1** (2) (2002) 133–144.
- [7] Chen, Z. and Williamson, A.C. Simulation study of a double three phase electric machine. *International Conference on Electric Ship*, September, 1998, 215–220, Istanbul, Turkey.
- [8] Habetler, T.G., Profumo, F., Griva, G., Pastorelli, M. and Bettini, A. Stator resistance tuning in stator flux field oriented drive using an instantaneous hybrid flux estimator. *Conf. Record EPE Conf. Brighton*, UK, **4** (1993) 292–299.
- [9] Hadiouche, D., Razik, H. and Rezzoug, A. Modeling on double star induction motor for space vector PWM control. *ICEM 2000* **1** 392–396, Finland.
- [10] Kerkman, R.J., Seibal, B.J., Rowan, T.M. and Sclegel, D. A new flux and stator resistance identifier for AC drive system. *Conf. Record, IEEE-IAS*, Orlando, Florida, 310–318, October 1995.
- [11] Lee, B.S. and Krishnan, R. Adaptive stator resistance compensator for high performance direct torque controlled induction motor drives *Conf. Record, IEEE-IAS* **1** (4) (1998) 423–430.
- [12] Liu, J., Wu, P.S., Bai, H.Y. and Huang, X. Application of fuzzy control in direct torque control of permanent magnet synchronous motor. In: *Proceeding of the 5th World Congress on Intelligent Control and Automation*, Hangzhou, P.R. China, 4573–4576, June 15-19, 2004.
- [13] Madani, N. Commande a structure variable d’une machine asynchrone double étoile alimentée par deux onduleurs MLI. *Thèse de doctorat de l’université de Nantes*, December 2004.

- [14] Malik, S.M., Eibuluk and Zinger, D.S. PI and fuzzy estimators for tuning the stator resistance in direct torque control of induction machine *IEEE Tran. on Power Electronics* **13** (2) (1998) 279–287.
- [15] Moubayed, N., Meibody-Tabar, F. and Davat, B. Alimentation par deux onduleurs de tension d'une machine synchrone double étoile *Revue Internationale de Génie Electrique (RIGE)* **1** (4) (1998) 457–470.
- [16] Nezli, L., Mahmoudi, M.O., Boucherit, M.S. and Djemai, M. On vector control of double star synchronous machine with current fed inverters *The Mediterranean Journal of Measurement and Control* **1** (3) (2005) 118–128.
- [17] Rasfsthain, T., Feuillet, R. and Perret, R. Double star synchronous machine modelisation. *Proc. of the 6th Conference on Power Electronics and Motion Control, PEMC'90*, 686–689.
- [18] Schiferl, R.F. and Ong, C.M. Six phase synchronous machine with AC and DC stator connections *IEEE Transaction on Power Apparatus and Systems* **PAS-102** (8) (1983) 2685–2693.
- [19] Sen, P.C. Electric motor drives and control — past present and future. *IEEE Transaction on Industrial Electronics* **37** (6) (1990) 562–575.
- [20] Terrien, F. Commande d'une machine synchrone double étoile, alimentée par deux onduleurs MLI. *Thèse de doctorat de l'université de Nantes*, December 2000.
- [21] Terrien, F. and Benkhoris, M.F. Modeling and study of double star alternative machine power electronic coverter-set. *ELECTRIMACS'99*, September 1999, **2** 201–206, Lisbonne, Portugal.
- [22] Van Hulse, J., Detemmerman, B., Buyse, H., Compere, M. and Thiry, J.M. A simplified analysis of damper losses and torque ripple of converter-fed, multiple armature polyphase synchronous machine. *ICEM*, September 1984 **2** 773–776, Lausanne (Switzerland).
- [23] Werren, L. Synchronous machine with 2 three phase winding, spatially displaced by 30°EL. Commutation reactance and model for converter-performance simulation. *ICEM*, September 1984 **2** 781–784, Lausanne (Switzerland).
- [24] Zhao, Y. and Lipo, T.A. Space vector PWM control of dual three-phase induction machine using vector space decomposition *IEEE Transactions on Industry Applications* **31** (5) (1995) 1100–1109.
- [25] Zong, L., Rahman, M.F., Hu, W.Y. and Lim, K.W. Analysis of direct torque control in permanent magnet synchronous motor drives *IEEE Transactions Power Electronics* **12** (3) (1997) 528–536.
- [26] Zong, L., Rahman, M.F., Hu, W.Y. and Lim, K.W. A direct torque controller for permanent magnet synchronous motor drives *IEEE Transactions on Energy Conversion* **14** (3) (1999) 637–642.